

Introduction

Heavy metals pose a serious threat to the environment, originating from diverse sources such as industrial discharge, refineries, and waste treatment facilities, as well as indirect pathways like soil, groundwater, and atmospheric deposition via rainfall.¹⁻⁶ Notable among these pollutants are cadmium (Cd), lead (Pb), and mercury (Hg), which exhibit toxicity even at low concentrations.^{7,8} Among them, Cd stands out as a significant global hazard,⁹⁻¹¹ presenting severe health risks to both human and wildlife populations. Its accumulation in plants leads to various physiological, biochemical, and structural alterations, affecting processes such as mineral nutrient absorption, photosynthesis, and carbohydrate metabolism, along with changes in antioxidant mechanisms.^{12,13} Therefore, effective environmental Cd removal methods are imperative, given the associated health risks and ecological implications. Current Cd remediation techniques include chemical precipitation, oxidation-reduction processes, ion-exchange, filtration, electrochemical treatments, reverse osmosis, evaporative recovery, and solvent extraction. However, these conventional methods face challenges such as unpredictable metal ion removal and the generation of potentially hazardous sludge. Therefore, there is a pressing need to develop more efficient, sustainable, and environmentally friendly Cd removal methods.^{14,15}

Bioremediation offers an alternative approach utilizing natural and engineered microorganisms to reduce or eliminate hazardous contaminants, including Cd.^{3,16,17} This method is recognized for its cost-effectiveness and environmentally friendly nature. Bacteria play a crucial role in bioremediating toxic metal ions. Particularly, *Pseudomonas aeruginosa* demonstrates notable Cd tolerance and applications in removing Cd and other heavy metals from various environments such as water, soil, contaminated waste, and solutions. *P. aeruginosa*, known for its resilience and adaptability, employs diverse mechanisms to resist Cd toxicity.¹⁸ Several studies have highlighted its ability to withstand Cd in different environmental conditions.^{3,16,17,19} These mechanisms include efflux pumps that actively expel Cd ions from the cell, reducing their intracellular accumulation, and utilizing metallothioneins, cysteine-rich proteins, to bind and sequester Cd ions, thereby minimizing their harmful effects. For instance, strains like *P. aeruginosa* KUCD1 and san ai²⁰ can tolerate high Cd concentrations, up to 8 mM,^{3,18} and 7.2 mM respectively, in nutrient agar medium at a pH of 7.2. Some *P. aeruginosa* species produce pyoverdine (PVD) under Cd stress, potentially aiding in reducing Cd accumulation in plants. In addition, *P. aeruginosa* PU21 biomass effectively removes Cd, Cu, and Pb from contaminated water. Similarly, the non-viable biomass of *P. aeruginosa* and strains isolated from active sludge exhibit robust adsorption abilities for Cd and Pb in aqueous solutions.³ Furthermore, adapted cells of *P. aeruginosa* and genetically engineered strains have been found effective in Cd removal.

Notably, *P. aeruginosa* BC15, an environmental isolate, displays resistance to Cd and can biosorb Cd as well as other metals like Pb, Ni, and Cr. Induction studies on *P. aeruginosa* BC15 using sub-lethal Cd concentrations have revealed the development of adaptive resistance to lethal Cd doses, further highlighting its potential in bioremediation efforts.^{3,18} This adaptive capability highlights the resilience of *P. aeruginosa* BC15 in confronting heavy metal stress. In addition, previous research underscores the efficacy of *P. aeruginosa* BC15 in mitigating Cd and Zn contamination in industrial wastewater and soil.^{3,18} The strain demonstrated notable resistance to these metals and exhibited substantial biosorption capacity, with Cd absorption reaching 82% and Zn reaching 85% in binary solutions. Furthermore, analysis of the Cd resistance (*cadR*) gene in *P. aeruginosa* BC15 revealed its similarity to other *Pseudomonas* strains. Cloning *cadR* into *E. coli* BL21 facilitated robust growth in Cd-supplemented media, indicating its potential for heavy metal remediation. Moreover, live cells of *Pseudomonas* BC15 displayed the ability to biosorb Cd, as well as other metals like Pb, Ni, and Cr, showcasing its versatility in metal detoxification. Overall, these findings highlight the potential of *P. aeruginosa* BC15 as a valuable tool in addressing heavy metal contamination in the environment.

In the intricate network of Cd resistance mechanisms in bacteria like *P. aeruginosa*, CadA stands as a frontline defender, orchestrating a timely response to Cd exposure.²¹ CadA is a membrane-bound efflux pump that actively expels Cd ions from the bacterial cell, reducing intracellular accumulation and mitigating toxicity.^{3,18,22} Its role extends beyond direct Cd efflux; it also triggers the induction of the *CzcCBA* efflux system, crucial for extruding multiple heavy metal ions from the bacterial cytoplasm, including Zn, Cu, and Cd. This coordinated response ensures the swift removal of Cd ions from the cellular milieu, safeguarding cellular integrity and functionality. *P. aeruginosa* possesses chromosomally encoded Cd resistance facilitated by 2 inversely transcribed genes, *cadR* and *cadA*. CadR, sourced from *P. aeruginosa*, encodes a transcriptional regulatory protein that exhibits a robust response to Cd(II), followed by Zn(II) and Hg(II), at its cognate promoter P_{cadA} . CadA shares structural similarities with Cd-transporting ATPases identified in Gram-positive bacteria.³ Functionality studies of CadA have referenced *E. coli* ZntA sequences.¹⁸⁻²⁰ Recent work by Kumari et al²³ unveiled the role of metal bioremediation mediated by CadC and CadA in the *B. megaterium* strain YC4-R4.

Furthermore, *CadA* plays a vital role in protecting bacterial cells from sudden surges in Zn levels, acting as a primary defense mechanism against Zn toxicity. The regulation of CadA expression is tightly controlled by the *CadR* transcriptional regulator, which orchestrates the cellular response to heavy metal exposure.^{18,24} In *P. aeruginosa*, the Cation-transporting P-type ATPases (*CadA*) protein is encoded by

the *cadA* gene, often located on genetic elements associated with heavy metal resistance, such as plasmids or genomic islands.¹⁸ This CadA protein serve as key players in cellular ion homeostasis and heavy metal resistance mechanisms. Understanding their function is essential for elucidating bacterial adaptation to metal-contaminated environments and developing strategies for environmental remediation and antimicrobial therapy. Research on CadA in *P aeruginosa*, a Cd resistance determinant, is essential due to its significance in understanding bacterial adaptation to heavy metal stress. Understanding the genomic context of the *cadA* gene is crucial for elucidating the regulatory networks and genetic pathways involved in Cd detoxification. Genomic analyses have identified neighbouring genes associated with Cd resistance or related cellular processes, providing insights into the genetic architecture of Cd tolerance in *P aeruginosa*.²⁵

Research on cation-transporting P-type ATPases sheds light on fundamental cellular processes and microbial adaptation to environmental challenges. These ATPases, crucial for mediating resistance to heavy metal ions like Cd, Cu, and Zn, offer avenues for combating antimicrobial resistance, enhancing metal bioremediation, and engineering microorganisms with improved metal tolerance. Understanding the structural basis and mechanisms governing CadA's cadmium binding affinity is vital for these advancements, holding promise for innovation in medicine, biotechnology, and environmental remediation.^{23,26} Recent research efforts have increasingly focused on computationally characterizing the active sites of proteins.^{27,28} This has led to the development of online resources dedicated to locating, delineating, and quantifying concave surface regions within 3D protein structures, enabling differentiation of metal resistance proteins. Physico-chemical attributes, including atom count, molecular weight, isoelectric point, and conserved domains, can be readily assessed.^{28,29} In addition, homology modelling and comparative proteomics approaches have been extensively employed to forecast the 3D structure, binding sites, and potential functionalities of metal regulatory proteins.^{30,31} However, the CadA protein and its binding capacity remain inadequately understood, with no prior reports elucidating its functional and structural attributes, including interactions with metals and metal complexes. Hence, this study endeavours to employ *in silico* methodologies for the identification and characterization of the 3D structures, metal binding proficiency, and removal mechanism of the cation-transporting P-type ATPase (CadA) in *Pseudomonas aeruginosa* BC15.

Experimental Section

Target sequence retrieval and phylogenetic analysis

The sequences for both nucleotide and protein of the CadA protein were obtained from the National Center for Biotechnology Information (NCBI) databases.³² It was observed that the *cadA* gene was positioned upstream of the

cadR promoter. To confirm this arrangement, the *cadR* gene (KU302252) was submitted to NCBI for further analysis, leading to the successful identification of the *cadA* gene. Subsequently, the specific nucleotide sequence of the *cadA* gene was retrieved from the NCBI database (<http://www.ncbi.nlm.nih.gov/>) by the accession number KU302252. Furthermore, the 2-dimensional structure of the heavy metals was acquired from the PUBCHEM database in SDF file format.

Investigation of template

The CadA protein sequences obtained were analyzed using the BLASTp algorithm within the standard protein BLAST suite. To conduct structural and functional analysis, both the CadA protein and gene sequences were sourced from the SWISS-PROT database. Sequences exhibiting noteworthy similarity were aligned through the ClustalW algorithm, integrated into the Molecular Evolutionary Genetic Analysis (MEGA 6) software, accessible at <http://www.megasoftware.net>. The alignment was further refined to generate a consensus sequence based on distance matrix analysis.

Examination of physicochemical characterization

Using the ProtParam tool, which is available at <http://web.expasy.org/protparam/>, the CadA protein in *P aeruginosa* BC15 underwent physicochemical characterization, including analysis parameters such as isoelectric point (pI), molecular weight, atom count, instability index, aliphatic index, and grand average of hydropathicity (GRAVY). Using CELLOv.2.5, subcellular localization was predicted. The PSIPRED server was used for secondary structure analysis, and the PRINTS server was used for fingerprint analysis.

Evaluation of CadA protein CDD and motif

The motif search tool (<http://www.genome.jp/tools/motif>) was employed to identify the conserved region within the CadA protein. In addition, the functional unit of the protein was annotated by the conserved domain database (<http://www.ncbi.nlm.nih.gov>). The secondary structure predictions were conducted by PDBsum (www.ebi.ac.uk/pdbsum), SOPMA server (<http://npsa-prabi-ibcp.fr/sopma.html>), and Phyre2 (www.sbg.bio.ic.ac.uk/phyre2). Protein-protein interactions were assessed using the STRING server.

Validation of CadA protein 3D structure modelling

The *cadA* gene encoded CadA protein sequences were retrieved from *P aeruginosa* (Uniprot ID: A0A0H2ZF06) in FASTA format and subjected to BLASTp evaluation against the PDB database for the identification of the suitable template for modelling. The SWISS MODEL tool, Phyre2, and RaptorX

Table 1. BLAST analysis of *cadA* gene from *Pseudomonas aeruginosa* BC15.

DESCRIPTION	SCORE	IDENTITY	ACCESSION NUMBER
<i>Pseudomonas putida</i> CadR (<i>cadR</i>) and CadA (<i>cadA</i>) genes	100%	98%	AF333961.1
<i>Pseudomonas putida</i> HB3267, complete genome	100%	97%	CP003738.1
<i>Pseudomonas monteilii</i> SB3101, complete genome	100%	96%	CP006979.1
<i>Pseudomonas monteilii</i> SB3078, complete genome	100%	96%	CP006978.1
<i>Pseudomonas</i> sp. DRA525 genome	100%	96%	CP018743.1
<i>Pseudomonas putida</i> strain DLL-E4, complete genome	100%	96%	CP007620.1
<i>Pseudomonas plecoglossicida</i> strain NyZ12, complete genome	100%	96%	CP010359.1
BLAST analysis of CadA protein from <i>Pseudomonas aeruginosa</i> BC15			
<i>Pseudomonas</i> sp	100%	99.86%	WP_116620229.1
<i>Pseudomonas oleovorans</i>	100%	99.73%	WP_074860391.1
<i>Pseudomonas chengduensis</i>	100%	98.65%	WP_017675921.1
<i>Pseudomonas pseudoalcaligenes</i>	100%	97.56%	WP_104729809.1
<i>Pseudomonas alcaliphila</i>	100%	97.43%	WP_075750492.1

servers were used to predict the 3D (3-dimensional) structure of CadA protein. The obtained model was visualized by SWISS MODEL (<http://www.expasy.org/spdbv>). The CadA protein 3D structure model quality was assessed using PyMOL, further validation was conducted by the Ramachandran plot analysis. QMEANZ score was calculated to evaluate and refine the predicted CadA protein model.

Analysis of the metal protein interactions by docking using PatchDock

In order to investigate interactions between metal-protein complexes, 2-dimensional structures of heavy metals (arsenate, cadmium, chromium, cobalt, copper, zinc, lead, silver, and nickel ions) were obtained from the PUBCHEM database in SDF file format. These structures were then converted to PDB file format using an online molecular converter tool (<http://cactus.nci.nih.gov/translate>). Docking analyses of the 3D structures were performed using the PatchDock tool, a molecular modelling simulation software known for its effectiveness in protein-ligand docking studies.

Results

Retrieval of target sequences (cadA gene) from Pseudomonas aeruginosa

The *cadA* gene sequence of *P. aeruginosa* BC15 was identified using *cadR* gene sequences. The *cadA* gene sequence was obtained in FASTA format with an accession number of NC_002516 (Figure S1A). Subsequently, the *cadA* gene sequence was subjected to the ExPASy Translate tool (<https://web.expasy.org/translate/>), resulting in the protein sequence AVZ34575.1, as shown in Figure S1B & C.

BLAST analysis of CadA protein from P aeruginosa BC15

The results of the BLAST analysis of the *cadA* gene from *P. aeruginosa* BC15 revealed a high degree of similarity with other *Pseudomonas* species. The analysis indicated that the *cadA* gene from *P. aeruginosa* BC15 had a 100% score and 98% identity with the CadR and CadA genes from *P. putida* HB3267, a 100% score and 96% identity with the genes from *P. monteilii* SB3101 and SB3078, a 100% score and 96% identity with the genes from *Pseudomonas* sp. DRA525, and a 100% score and 96% identity with the genes from *P. putida* and *P. plecoglossicida* (Figure S2). The BLAST analysis of the CadA protein from *P. aeruginosa* BC15 also revealed a high degree of similarity with other *Pseudomonas* species. The analysis indicated that the CadA protein from *P. aeruginosa* BC15 had a 100% score and 99.86% identity while the CadA protein from *Pseudomonas* sp., and a 100% score and 99% identity (Table 1).

Phylogenetic distribution and evolutionary relationship of cadA gene and CadA protein

The phylogenetic trees were constructed by Neighbour-joining method using *cadA* gene and its protein sequences of *Pseudomonas aeruginosa*. The phylogenetic tree of *cadA* gene and its protein sequences showed the evolutionary relationship between strains *Pseudomonas* genera (Figure 1).

Physicochemical parameters

The physicochemical parameters were analysed using the ProtParam tool. The CadA protein was predicted to consist of 690 amino acids with a molecular weight of 73 352.85 Daltons

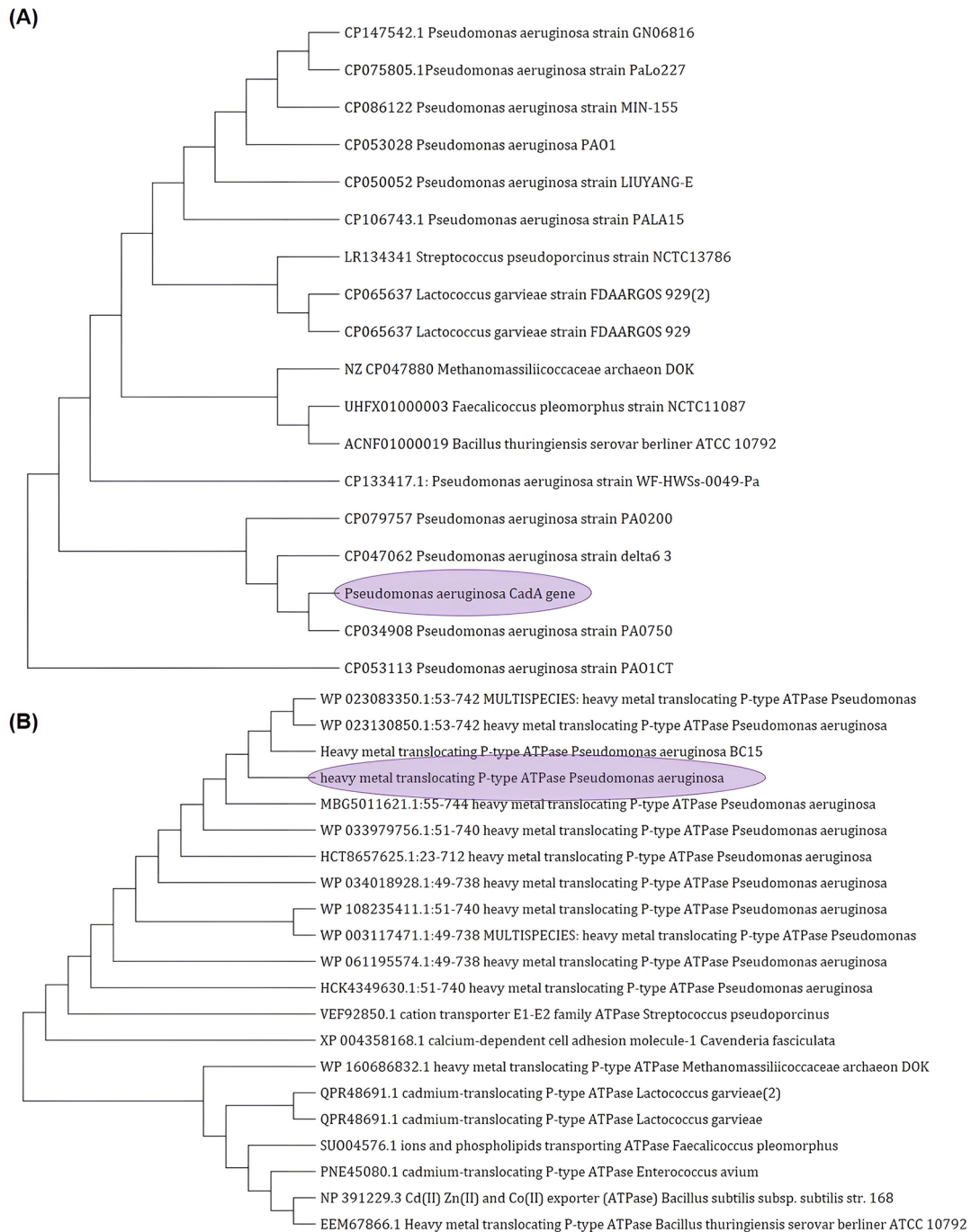


Figure 1. Phylogenetic analysis of the *cadA* gene and its protein across *Pseudomonas* species and gram-positive bacteria. (A) Evolutionary relatedness of the *cadA* gene sequences from *Pseudomonas aeruginosa* (highlighted) compared to homologous sequences from other *Pseudomonas* species and gram-positive bacteria. The phylogenetic tree demonstrates the genetic divergence and common ancestry among these *cadA* gene sequences. (B) Phylogenetic tree depicting the evolutionary relationship of the CadA protein sequences from *P. aeruginosa* (highlighted) in comparison to related proteins from other *Pseudomonas* species and gram-positive bacteria. The analysis highlights the conservation and divergence of CadA protein sequences across these bacterial taxa.

and a theoretical isoelectric point (pI) of 5.39. The amino acid composition revealed that alanine comprised the highest percentage at 14.8%, followed by leucine at 13.8%, arginine at 6.7%, and other amino acids occurring in less than 9% abundance. A total of 80 residues were negatively charged, while 66

residues were positively charged. The instability index (II) was calculated to be 31.60, and the aliphatic index was determined to be 113.20. The grand average of hydropathicity (GRAVY) was found to be 0.241 (Table 2). Subcellular localization analysis predicted the target CadA protein to be present in the

Table 2. The physicochemical properties of the CadA protein.

AMINO ACID COMPOSITION	AMINO ACIDS	RESIDUES	%
	Alanine (A)	102	14.8
	Arginine (R)	46	6.7
	Asparagine (N)	16	2.3
	Aspartic acid (D)	37	5.4
	Cysteine (C)	5	0.7
	Glutamine(Q)	21	3.0
	Glutamic acid(E)	43	6.2
	Glycine (G)	61	8.8
	Histidine (H)	10	1.4
	Isoleucine (I)	36	5.2
	Lysine (L)	95	13.8
	Lys(K)	20	2.9
	Methionine (M)	12	1.7
	Phenylalanine (F)	17	2.5
	Proline (P)	33	4.8
	Serine (S) s	29	4.2
	Threonine (T)	32	4.6
Molecular weight	73352.85		
Theoretical pI	5.39		
Instability index	31.60		
Aliphatic index	113.20		
Grand average of hydropathicity(GRAVY)	0.241		
Number of –vely charged amino acids (R + L)	80		
Total number of positively charged residues (Arg + Lys)	66		
Types of atoms present in the CadA protein	C 3275 (Carbon) H 5320 (Hydrogen) Nitrogen N 916 Oxygen O 955 Sulphur S 17		
Valued half-life:	Predictable half-life is: Approximately 30 hours in mammalian reticulocytes <i>in vitro</i> . Over 20 hours in yeast, <i>in vivo</i> . More than 10 hours in <i>Escherichia coli</i> , <i>in vivo</i> .		
Formula	C3275H5320N916O955S17		

cytoplasm (value 2.493) as determined by CELLOv2.5. Secondary structure analysis of the CadA protein identified parameters such as alpha helix and random coil using PSIPRED (Figure S3B). The fingerprint predictor from the

PRINTS server revealed that the CadA protein contains 2 fingerprints: CATATPASE, which consists of 5 out of 6 motif numbers, and CDATPASE, which contains 3 out of 9 motifs.

Conserved domain and motif analysis

The 5 conserved domains/functional motifs in CadA were analysed using Motif Finder (Figure S3A). The aligned sequences of a consanguineous protein family were examined using the SOPMA algorithm. Each sequence line was visually labelled with colour-coded predictions for helix, sheet, turns, and coils. The proportions of alpha helix and beta strand were determined by SOPMA using a homology-based technique. The identification of beta turns, important secondary structure components, greatly aided in the formation of an interim stage. These beta turns were also observed in the secondary structure, contributing to the formation of an intermediate structure that eventually folds into a 3-dimensional structure (Figure S4). Protein-protein interactions of the CadA protein were evaluated using the STRING database. The resulting coloured lines indicate different sources of evidence for each interaction within the proteins (Figure S5).

Conserved domain analysis by Clustal Omega

The other MerR cation transport ATPase proteins of *Pseudomonas* sp. were analysed through multiple sequence alignment. Clustal Omega was utilized for aligning the selected protein sequences. The multiple sequence alignment results revealed the conservation of amino acid residues from the *Pseudomonas* sp. *cadA* gene (Figure 2). Hydrophobic amino acids are represented in green, polar ones in blue, aliphatic residues in black, and positively charged amino acids in red.

Homology modelling was employed using the SWISS-MODEL software to construct the 3D structure of CadA. The primary sequence of CadA was obtained from UniProt, and template searching was conducted using SWISS-MODEL software. Figure 2B illustrates the selection process, where the crystallographic structure of *E coli* CopA (PDB code 3J09), resolved via X-ray method at a resolution of 1.30 Å, was chosen as the template due to its highest sequence identity of 33.73% with the target sequence among 50 given templates. The final 3D structure was obtained from the SWISS-MODEL software and utilized for subsequent docking studies. Overall, the evaluation suggests that the predicted CadA model exhibits satisfactory stability and warrants further analysis (Figure 2C).

Phyre2

In the Phyre results, matching residues between the query and template are shaded with a gray background. Predicted and confirmed secondary structures are delineated as α -helices. Conservation levels for both the query (CadA) and template sequences are represented by horizontal bars, with thicker bars denoting greater conservation. The 'Conservation' rows classify residue conservation into 3 states. No symbol indicates lack of conservation, a thin gray bar suggests moderate conservation, and a large block signifies a high degree of conservation. Details

regarding confidence lines can be found in the Secondary Structure and Disorder section. Alpha helices are depicted in green, beta strands in blue, and random coil with faint lines. The 'SS confidence' line indicates the level of confidence in the prediction, with red signifying high confidence and blue indicating lower confidence. Phyre generates a series of 3D protein models through structural alignment. In addition, it identifies sequence homologues using PSI-BLAST (Figure 3).

Model validation, energy minimization, and 3-dimensional structure modelling

Homology modelling was conducted using SWISS-MODEL. The sequence of the CadA protein underwent a BLASTp search against the PDB database to identify the closest matching crystal structure, which was then utilized as a template for modelling the target protein. The SWISS-MODEL server identified the PDB ID 3J09 (CopA protein) as a suitable template with 33.73% identity (Figure S6). The examination of the Ramachandran plot revealed that 89.3% of the residues occupied the favoured (red) region, with 7.3% falling within the allowed (blue) region, while the remaining 3.4% of residues were situated in either the generously allowed (yellow) or outlier region. The presence of over 89.3% of residues in the favoured region suggests the acceptability of the model (Figure 4A). The QMEAN value was determined to be -4.91 (Figure 4B and C). The structure was visualized, and docked complexes were analysed using PyMOL (Figure 4D).

Docking analysis

The docking analysis, 3D structure of CadA protein was carried out by PatchDock. The 2D structures of heavy metal ions including Cadmium, Arsenic, Chromium, Cobalt, Copper, Nickel, Lead, Silver, Zinc, and Cadmium chloride were acquired from PUBCHEM in SDF format. Subsequently, they were transformed into PDB file format using an online molecular conversion tool at <http://cactus.nci.nih.gov/translate/>. (Figure S8). Target protein 3D structure of CadA bound Cd complex was visualized in PyMOL (Figure S7). Figure 5 show the protein-ligand interaction of CadA and heavy metals complexes. The binding of Cd with the E101 and H96 residues in the catalytic site indicated that the CadA protein is responsible for Cd detoxification in *P aeruginosa*. The result of the PatchDock analysis also supported that CadA has higher affinity to CdSO₄ than other heavy metals based on the Atomic contact energy (ACE), Score and area values such as, -58.03 Kcal/Mol, 1702, 172.70 respectively (Table 3). PatchDock values of other heavy metals binding with CadA are shown in Figure 5.

Discussion

Heavy metal contamination is a severe problem that results in the deterioration of human health. Specifically, cadmium (Cd)

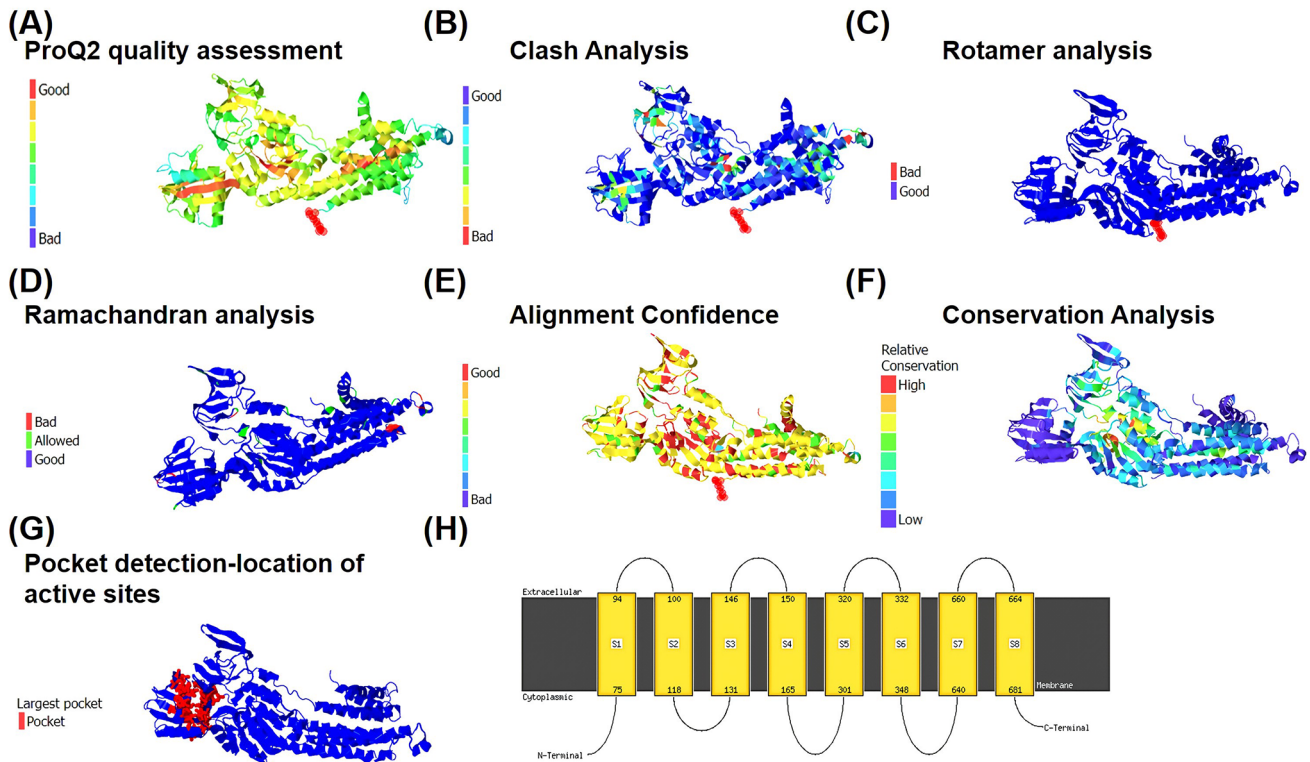


Figure 3. Validation of CadA protein 3D structure by Phyre2. (A) Model quality assessment by ProQ2. The colour gradient indicates the reliability of the model, with red regions representing areas of low confidence and blue regions indicating higher confidence. (B) Clash analysis of CadA protein. The colour gradient represents clash severity, where blue regions denote minimal clashes and red regions signify significant clashes. (C) Analysis of rotamers. The colour gradient reflects the quality of rotamer conformations, with blue regions indicating well-packed and favourable conformations, and red regions representing unfavourable conformations. (D) Ramachandran analysis for CadA protein. The colour gradient represents the distribution of phi-psi angles, with blue regions indicating favourable backbone conformations and red regions representing outliers. (E) Alignment confidence from HHsearch. The colour gradient is reversed, with red regions indicating higher confidence in the alignment and blue regions representing lower confidence. (F) Detection of sequence features using the Conserved Domain Database (CDD). The colour gradient signifies conservation levels, with red regions indicating highly conserved regions and blue regions representing less conserved areas. (G) Pocket detection by fpocket2. The largest pocket of the active site is highlighted in red. (H) Transmembrane helices of CadA protein. 615 residues (89% of CadA sequence) have been modelled with 100.0% confidence by the single highest-scoring template.

is an extremely toxic heavy metal for the environment, causing diseases such as itai-itai disease, cancers, osteoporosis, lung disease, and atherosclerosis in human.^{1,29,30} Studies have reported that Cd contamination in soil and drinking water has increased several times in many parts of the world. To control and remediate Cd contamination, a number of chemical and traditional methods are used. However, these methods have major disadvantages; they are more expensive and produce secondary compounds that are even more toxic.^{31,32}

Therefore, an alternative biological method of Cd bioremediation is needed. The expression of Cd tolerance genes, under the regulation of CadA proteins, confers tolerance to Cd. In particular, *Pseudomonas aeruginosa*, a Cd-resistant bacterium isolated from industrial effluent wastewater, plays a major role in Cd removal using *cadA* and *cadR* genes, which encode P-type ATPase (CadA) and transcript regulatory protein (CadR). Moreover, *P. aeruginosa* exhibits elevated Cd resistance capabilities, nearly 7.2mM³, in contrast to other organisms,

attributed to the presence of *cadA* and *cadR* genes along with their respective proteins. Although the role of CadA has been described in previous studies, little has been discovered regarding the CadA 3D structure's metal recognition and binding properties. In the current scenario, protein homology modeling was used for the prediction of the 3D structure of the unknown protein by known protein structure. Therefore, this study is aimed at identifying and characterizing the cation-transporting P-type ATPase (*cadA*) in *P. aeruginosa* BC15 through *in silico* methods.

The identified and retrieved *cadA* gene sequence was used for NCBI BLAST analysis. Local alignment (BLASTp) and global alignment (Clustal Omega) were utilized to determine both near and distant relationships of the CadA protein with other species. BLASTp identified segments of the sequence that are conserved among other organisms, while Clustal Omega provided a more detailed analysis, displaying similarities among analogous sequences of amino acids of each com-

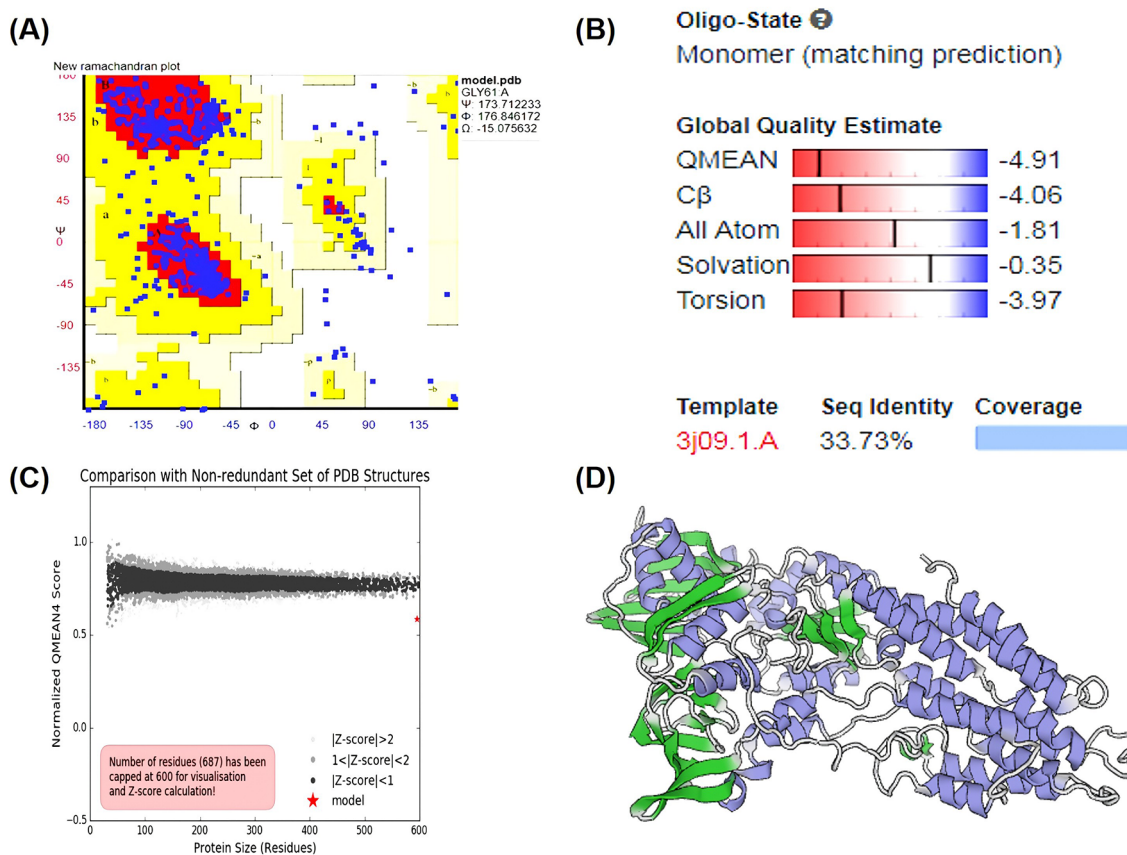


Figure 4. Energy minimization and validation of the model. (A) The Ramachandran plot illustrates the distribution of psi/phi values for the CadA protein. The colour legend denotes regions of varying favourability: red for the most favoured, yellow for allowed, pale yellow for generously allowed, and white for disallowed regions. (B) A graph compares the protein size with a non-redundant set of PDB structures, normalized for analysis. (C) The QMEAN4 score provides an assessment of the model's quality, indicated by a red star. Models with Z-scores exceeding 2 are shaded in light gray. The red star represents the model. (D) The dimeric model of the CadA protein from *Pseudomonas aeruginosa* is depicted in cartoon form. The DNA and metal binding domains are also annotated. The 3D structure of the CadA protein model was visualized using PYMOL.

pared protein. The sequence alignment of CadA from *P. aeruginosa* BC15 clearly depicted conserved residues in other organisms. Conservation results obtained from Clustal Omega revealed highly conserved amino acid sequences with gap-free regions. In addition, a phylogenetic tree was constructed for the *cadA* gene-encoded CadA protein from *P. aeruginosa* BC15, based on amino acid sequences, revealing the evolutionary relationship of *Pseudomonas* sp., which is consistent with earlier reports documented in the NCBI database.

Physicochemical properties were analysed using the ProtParam tool. The analysis revealed that the CadA protein contains 14% alanine, 6.7% arginine, and other amino acids occurring in minimal percentages. Conserved amino acid regions were identified through motif analysis, employing the Conserved Domain Database search targeting sequences, superfamilies, and functional sites. Results from the PRINTS server indicated that CadA contains 2 fingerprints: CATATPASE, which has 5 out of 6 motifs, and CDATPASE, which has 3 out of 9 motifs. Secondary structure analysis performed by the SOPMA server showed 51.52% (355/689)

alpha helix, 7.11% beta turn, 27.43% random coil, and 13.93% extended strand. These findings are consistent with the results reported by Rajkumar et al.¹⁸

The research underscores the importance of understanding the 3-dimensional structure of proteins, particularly in fields like enzyme kinetics, ligand-protein interactions, and structure-based molecular compound design.^{18,20} By employing homology modelling techniques,³³⁻³⁷ the study successfully constructed the 3D structure model of the CadA protein using 3J09 as a template structure. Validation of the CadA protein structure through RAMPAGE revealed that 98% of its amino acid residues were located in the most favoured region, indicating the reliability of the model. This aligns with findings from Rajkumar et al,¹⁸ which reported similar validation results for protein models.

In the context of bioremediation, metal sulfide precipitation emerges as a superior technique due to several advantages over conventional methods such as hydroxide, carbonate, or phosphate precipitation. It not only reduces sludge volume but also forms compounds with lower solubility products, enabling the

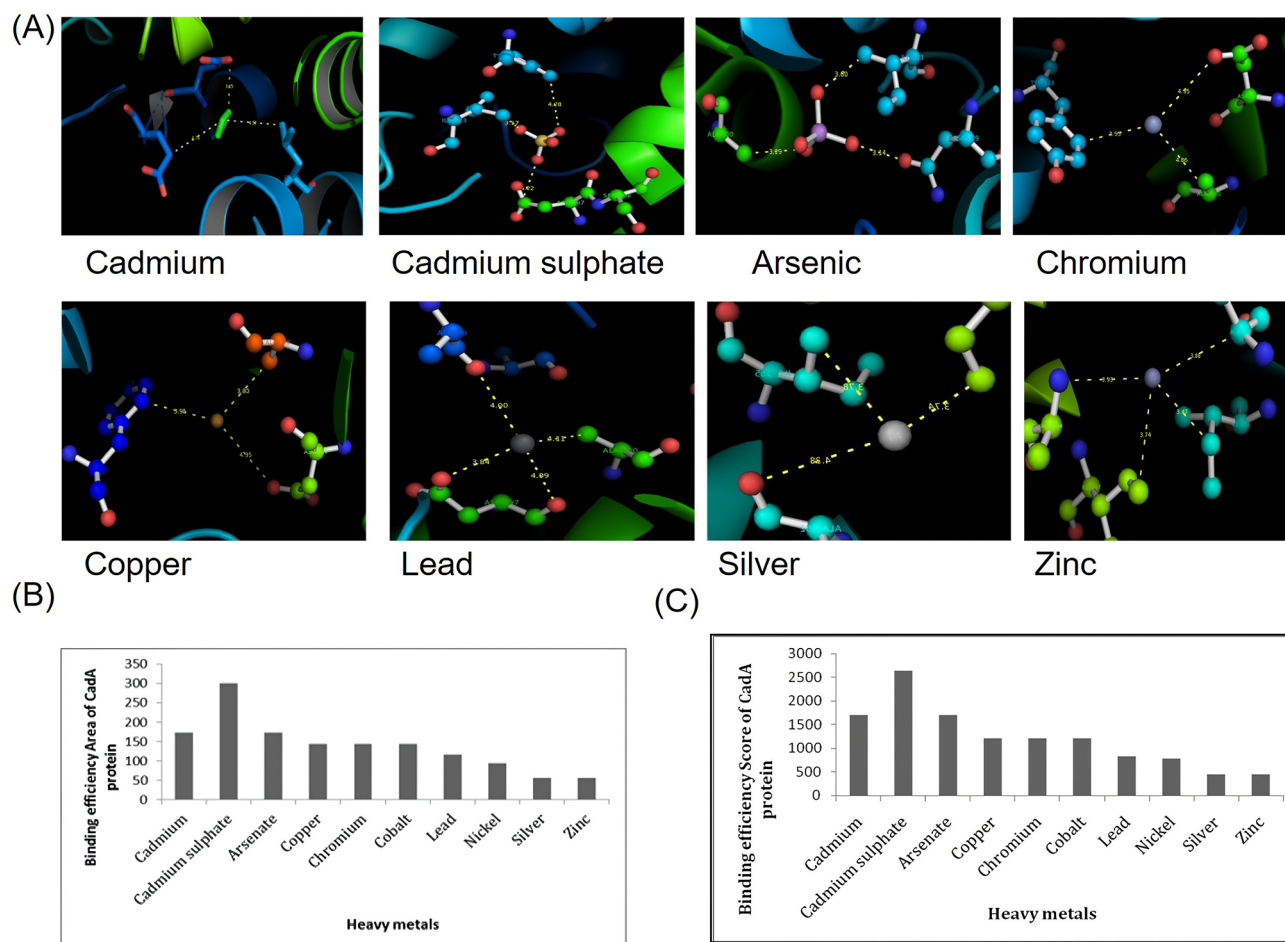


Figure 5. Illustrates the results of PatchDock analysis conducted to examine the interaction between the CadA protein and various heavy metals, including cadmium, cadmium sulfate, arsenate, copper, chromium, cobalt, lead, nickel, silver, and zinc. (A) displays the predicted binding areas of the CadA protein with each heavy metal. (B) presents the binding efficiency scores of the CadA protein with the aforementioned heavy metals. (C) These analyses provide insights into the potential affinity and interaction strength between the CadA protein and different heavy metal ions, which are crucial for understanding the protein's role in metal binding and detoxification processes.

Table 3. CadA binding efficiency with heavy metals.

HEAVY METALS	SCORE	AREA	ATOMIC CONTACT ENERGY
Cadmium	1702	172.70	-58.03
Cadmium sulfate	2636	300.10	-94.83
Arsenic	1700	173.60	-12.92
Chromium	1212	143.60	-17.74
Copper	1212	143.60	-17.74
Lead	818	116.70	24.61
Silver	440	55.80	0.00
Zinc	440	55.80	0.00

recovery of valuable metals. Among the heavy metals targeted for remediation, cadmium sulfate (CdSO_4) is particularly noteworthy for its stability and insolubility, making it an ideal

candidate for remediation efforts. CdSO_4 finds extensive use in various industries, including electroplating, pigments, batteries, and catalysis, underscoring its significance. However, the potential hazards associated with CdSO_4 exposure, as evidenced by studies by Yorulmazlar et al³⁷ and Yin et al,³⁸ have highlighted the toxic effects of CdSO_4 exposure, particularly when combined with other substances like α -naphthoflavone (ANF), leading to increased oxidative stress and down-regulation of protective genes in zebrafish embryos. These findings underscore the urgent need for effective bioremediation strategies targeting cadmium sulfate contamination to mitigate its adverse effects on the environment and human health. To address this need, PatchDock analysis was employed to predict the binding ability of the target CadA protein with different heavy metals, including arsenite, arsenate, arsenic, zinc, cadmium, copper, lead, cobalt, and silver. The analysis revealed that the CadA protein exhibits a higher binding affinity to Cd and CdSO_4 compared to other heavy metals, with a binding score of -58.03 kcal/mol (ACE). Correspondingly, Bai et al³⁹ found

out that most of the cadmium was removed by making cadmium sulfide through bioprecipitation, and only a little was taken out by biosorption.

In our study, we investigated the amino acid composition of the CadA protein, revealing notable proportions of alanine (A) and arginine (R), among others. These amino acids likely play critical roles in CadA's interaction with cadmium sulfate. Specifically, alanine's aliphatic nature facilitates hydrophobic interactions with metal ions, while arginine's positively charged side chain enables electrostatic interactions with negatively charged groups in cadmium sulfate. Moreover, the physicochemical properties of CadA provide insights into its structural stability, which is essential for metal binding processes. As a P-type ATPase, CadA is implicated in active transport across membranes, potentially including the transport of Cd ions. This suggests its involvement in cadmium sulfate removal or detoxification within the cell. Furthermore, the identification of conserved regions and domains within CadA, along with its evolutionary conservation, underscores its significance in metal tolerance mechanisms across species. Thus, CadA likely plays a pivotal role in binding and removing cadmium ions, including those from cadmium sulfate, thereby aiding in heavy metal stress mitigation. The observed higher affinity of CadA from *Pseudomonas* for CdSO₄ compared to Cd ions holds implications for cellular function and bioremediation strategies. Given CdSO₄'s stability and insolubility, its efficient removal poses a significant challenge. However, CadA's preferential binding to CdSO₄ suggests a specialized mechanism for Cd sequestration and detoxification within the cell, potentially offering a targeted approach to remediation. Leveraging CadA's cadmium-binding capabilities could lead to innovative bioremediation technologies tailored for CdSO₄ removal, thereby advancing environmental cleanup efforts and mitigating contamination risks. Overall, CadA's affinity for CdSO₄ represents an intriguing adaptation with promising implications for both cellular function and environmental remediation, warranting further exploration of its molecular mechanisms and biotechnological applications.

Conclusions

In conclusion, this study identifies the *CadA* gene from *Pseudomonas aeruginosa* BC15, characterizing its high homology with related proteins and evaluating its physicochemical parameters and structural stability. Molecular docking studies reveal CadA's preference for binding cadmium, highlighting its potential role in Cd tolerance mechanisms and bioremediation. This work contributes to understanding CadA's 3D structure and its affinity for metal cations, paving the way for future research on Cd monitoring and environmental remediation strategies.

Author Contributions

T.R.K. conducted the experimental work, while P.R.K., as the corresponding author and research team supervisor, oversaw

the experimental design, compilation, and revision of the full-length article.

ORCID iD

Rajkumar Prabhakaran  <https://orcid.org/0000-0002-7786-2034>

SUPPLEMENTAL MATERIAL

Supplemental material for this article is available online.

REFERENCES

- Masindi V, Muedi KL. Environmental contamination by heavy metals. *Heavy Metals*. 2018;10:115-132.
- Ashrafi E, Alemzadeh A, Ebrahimi M, Ebrahimi E, Dadkhodaei N, Ebrahimi M. Amino acid features of PIB-ATPase heavy metal transporters enabling small numbers of organisms to cope with heavy metal pollution. *Bioinform Biol Insights*. 2011;5:59-82.
- Chelliah ER. Cadmium (heavy metals) bioremediation by *Pseudomonas aeruginosa*: a minireview. *Appl Water Sci*. 2018;8:1-10.
- Vijayaraghavan K, Yun Y-S. Bacterial biosorbents and biosorption. *Biotechnol Adv*. 2008;26:266-291.
- Sonone SS, Jadhav S, Sankhla MS, Kumar R. Water contamination by heavy metals and their toxic effect on aquaculture and human health through food chain. *Lett Appl Nanobiosci*. 2020;10:2148-2166.
- Shuaib M, Azam N, Bahadur S, Romman M, Yu Q, Xuexiu C. Variation and succession of microbial communities under the conditions of persistent heavy metal and their survival mechanism. *Microb Pathog*. 2021;150:104713.
- Rahman Z, Singh VP. The relative impact of toxic heavy metals (THMs) (arsenic (As), cadmium (Cd), chromium (Cr)(VI), mercury (Hg), and lead (Pb)) on the total environment: an overview. *Environ Monit Assess*. 2019;191:1-21.
- Encarnaç o T, Pais AA, Campos MG, Burrows HD. Endocrine disrupting chemicals: impact on human health, wildlife and the environment. *Sci Prog*. 2019;102:3-42.
- Paul S, Dey S, Kundu R. Genomics and genetic engineering to develop metal/metalloid stress-tolerant rice. In: Roychoudhury, A, ed. *Rice Research for Quality Improvement: Genomics and Genetic Engineering: Volume 1: Breeding Techniques and Abiotic Stress Tolerance*. Springer; 2020:327-356.
- Lanza MGDB, Reis ARD. Roles of selenium in mineral plant nutrition: ROS scavenging responses against abiotic stresses. *Plant Physiol Biochem*. 2021;164:27-43.
- Khanna K, Kohli SK, Ohri P, Bhardwaj R, Ahmad P. Agroecotoxicological aspect of Cd in soil-plant system: uptake, translocation and amelioration strategies. *Environ Sci Pollut Res Int*. 2022;29:30908-30934.
- Chai WS, Cheun JY, Senthil Kumar P, et al. A review on conventional and novel materials towards heavy metal adsorption in wastewater treatment application. *J Clean Prod*. 2021;296:126589.
- Tamjidi S, Ameri A. A review of the application of sea material shells as low cost and effective bio-adsorbent for removal of heavy metals from wastewater. *Environ Sci Pollut Res Int*. 2020;27:31105-31119.
- Babiker RA, Elsharief UA, Salim JB, Mohammed NAR, Abdallah HM. Bacterial removal of lead and mercury elements from water using *Pseudomonas aeruginosa* in vitro. *Appl Microbiol Open Access*. 2020;6:169.
- Vishnoi N, Dixit S. Bioremediation: new prospects for environmental cleaning by fungal enzymes. In: Yadav A, Singh S, Mishra S, et al., eds. *Recent Advancement in White Biotechnology Through Fungi*. Springer; 2019:17-52.
- Vieto S, Rojas-G atjens D, Jim enez JI, Chavarr a M. The potential of *Pseudomonas* for bioremediation of oxyanions. *Environ Microbiol Rep*. 2021;13:773-789.
- Jagannathan SV, Manemann EM, Rowe SE, Callender MC, Soto W. Marine actinomycetes, new sources of biotechnological products. *Mar Drugs*. 2021;19:365.
- Prabhakaran R, Rajkumar SN, Ramprasad T, Selvam GS. Identification of promoter PcadR, in silico characterization of cadmium resistant gene cadR and molecular cloning of promoter PcadR from *Pseudomonas aeruginosa* BC15. *Toxicol Ind Health*. 2018;34:819-833.
- Tsai K-J. *Biochemical Characterization of the cadA Cadmium Resistance Determinant from Staphylococcal Plasmid pI258* [dissertation]. Detroit, MI: Wayne State University; 1994.
- Izrael-Zivkovi c L, Rikalovi c M, Gojgi c-Cvijovi c G, et al. Cadmium specific proteomic responses of a highly resistant *Pseudomonas aeruginosa* strain. *RSC Adv*. 2018;8:10549-10560.

21. Bazzi W, Abou Fayad AG, Nasser A, et al. Heavy metal toxicity in armed conflicts potentiates AMR in *A. baumannii* by selecting for antibiotic and heavy metal co-resistance mechanisms. *Front Microbiol.* 2020;11:68.
22. Ducret V, Gonzalez MR, Leoni S, Valentini M, Perron K. The CzcCBA efflux system requires the CadA P-type ATPase for timely expression upon zinc excess in *Pseudomonas aeruginosa*. *Front Microbiol.* 2020;11:911.
23. Kumari WMNH, Thiruchittampalam S, Weerasinghe MSS, Chandrasekharan NV, Wijayarathna CD. Characterization of a *Bacillus megaterium* strain with metal bioremediation potential and in silico discovery of novel cadmium binding motifs in the regulator, CadC. *Appl Microbiol Biotechnol.* 2021;105:2573-2586.
24. Brocklehurst K, Megit SJ, Morby AP. Characterisation of CadR from *Pseudomonas aeruginosa*: a Cd (II)-responsive MerR homologue. *Biochem Biophys Res Commun.* 2003;308:234-239.
25. Tetaz TJ, Luke RK. Plasmid-controlled resistance to copper in *Escherichia coli*. *J Bacteriol.* 1983;154:1263-1268.
26. Bhagwat G, Zhu Q, O'Connor W, et al. Exploring the composition and functions of plastic microbiome using whole-genome sequencing. *Environ Sci Technol.* 2021;55:4899-4913.
27. Kumar SU, Rajan B, Kumar DT, et al. Comparison of potential inhibitors and targeting fat mass and obesity-associated protein causing diabetes through docking and molecular dynamics strategies. *J Cell Biochem.* 2021;122:1625-1638.
28. Ullah A, Ul Qamar MT, Nisar M, et al. Characterization of a novel cotton MYB gene, GhMYB108-like responsive to abiotic stresses. *Mol Biol Rep.* 2020;47:1573-1581.
29. Rubalakshmi G, Vijayakumar N, Prabhakar YK, et al. Analysis of *Diplocyclos palmatus* plant biomaterials (proteins) using in silico approach and homology modeling [published online ahead of print October 24, 2020]. *Mater Today Proc.* doi:10.1016/j.matpr.2020.09.435
30. Zhao J, Cao Y, Zhang L. Exploring the computational methods for protein-ligand binding site prediction. *Comput Struct Biotechnol J.* 2020;18:417-426.
31. Abbas SZ, Rafatullah M, Hossain K, Ismail N, Tajarudin HA, Abdul Khalil HPS. A review on mechanism and future perspectives of cadmium-resistant bacteria. *Int J Environ Sci Technol.* 2018;15:243-262.
32. Fatima G, Raza AM, Hadi N, Nigam N, Mahdi AA. Cadmium in human diseases: it's more than just a mere metal. *Indian J Clin Biochem.* 2019;34:371-378.
33. Sievers F, Higgins DG. Clustal Omega, accurate alignment of very large numbers of sequences. In: Russell D, ed. *Multiple Sequence Alignment Methods.* Humana Press; 2014:105-116.
34. Gasteiger E, Hoogland C, Gattiker A, et al. Protein identification and analysis tools on the ExPASy server. In: Walker JM, ed. *The Proteomics Protocols Handbook.* Humana Press; 2005:571-607.
35. Studer G, Tauriello G, Bienert S, Biasini M, Johner N, Schwede T. ProMod3 – A versatile homology modelling toolbox. *PLoS Comput Biol.* 2021;17:e1008667.
36. Studer G, Rempfer C, Waterhouse AM, Gumienny R, Haas J, Schwede T. QMEAND is Co-distance constraints applied on model quality estimation. *Bioinformatics.* 2020;36:1765-1771.
37. Yorulmazlar E, Gül A. Investigation of acute toxicity of cadmium sulfate (CdSO₄·H₂O) and behavioral changes of grass carp (*Ctenopharyngodon idellus* Val., 1844). *Chemosphere.* 2003;53:1005-1010.
38. Yin J, Yang JM, Zhang F, Miao P, Lin Y, Chen ML. Individual and joint toxic effects of cadmium sulfate and α -naphthoflavone on the development of zebrafish embryo. *J Zhejiang Univ Sci B.* 2014;15:766-775.
39. Bai HJ, Zhang ZM, Yang GE, Li BZ. Bioremediation of cadmium by growing *Rhodobacter sphaeroides*: kinetic characteristic and mechanism studies. *Biore-sour Technol.* 2008;99:7716-7722.